Published in final edited form as:
J Immunol. 2009 December 1; 183(11): 6989–6997. doi:10.4049/jimmunol.0901386.

Role of double-stranded RNA pattern recognition receptors in rhinovirus-induced airway epithelial cell responses

Qiong Wang[1], **Deepti R. Nagarkar**[1], **Emily R. Bowman**[2], **Dina Schneider**[2], **Babina Gosangi**[2], **Jing Lei**[2], **Ying Zhao**[2], **Christina L. McHenry**[2], **Richai V. Burgens**[2], **David J. Miller**[3], **Umadevi Sajjan**[2], and **Marc B. Hershenson**[1,2]

[1]Department of Molecular and Integrative Physiology, University of Michigan, Ann Arbor

[2]Department of Pediatrics and Communicable Disease, University of Michigan, Ann Arbor

[3]Department of Internal Medicine, University of Michigan, Ann Arbor

Abstract

Rhinovirus (RV), a single-stranded RNA virus of the picornavirus family, is a major cause of the common cold as well as asthma and chronic obstructive pulmonary disease exacerbations. Viral double-stranded RNA produced during replication may be recognized by the host pattern recognition receptors Toll-like receptor (TLR)-3, retinoic acid inducible gene (RIG)-I and melanoma-differentiation-associated gene (MDA)-5. No study has yet identified the receptor required for sensing RV double-stranded (ds)-RNA. To examine this, BEAS-2B human bronchial epithelial cells were infected with intact RV-1B or replication-deficient UV-irradiated virus, and interferon (IFN) and IFN-stimulated gene expression determined by quantitative PCR. The separate requirements of RIG-I, MDA5 and IFN response factor (IRF)-3 were determined using their respective siRNAs. The requirement of TLR3 was determined using siRNA against the TLR3 adaptor molecule TRIF. Intact RV-1B, but not UV-irradiated RV, induced IRF3 phosphorylation and dimerization, as well as mRNA expression of IFN-β, IFN-λ1, IFN-λ2/3, IRF7, RIG-I, MDA5, IP-10/CXCL10, IL-8/CXCL8 and GM-CSF. siRNA against IRF3, MDA5 and TRIF, but not RIG-I, decreased RV1B-induced expression of IFN-β IFN-λ1, IFN-λ2/3, IRF7, RIG-I, MDA5 and IP-10/CXCL10, but had no effect on IL-8/CXCL8 and GM-CSF. siRNAs against MDA5 and TRIF also reduced IRF3 dimerization. Finally, in primary cells, transfection with MDA5 siRNA significantly reduced IFN expression, as it did in BEAS-2B cells. These results suggest that TLR3 and MDA5, but not RIG-I, are required for maximal sensing of RV dsRNA, and that TLR3 and MDA5 signal through a common downstream signaling intermediate, IRF3.

Keywords

Innate immunity; interferon; MDA5; RIG-I; TLR3

Introduction

Viral infections, most commonly caused by rhinovirus (RV), are a frequent cause of asthma and chronic obstructive pulmonary disease exacerbations (1). RV is a non-enveloped, positive, single-stranded RNA virus from the *Picornaviridae* family. RV is internalized by

*Address correspondence to: Marc B. Hershenson, M.D., University of Michigan, 1150 W., Medical Center Dr., Room 3570, MSRBII, Box 5688, Ann Arbor, MI USA 48109-0688. Phone: (734) 936-4200; FAX: (734) 764-3200; mhershen@umich.edu.

receptor-mediated endocytosis and undergoes a conformational change at endosome low pH, leading to insertion of viral RNA into the cytosol. After entry, replication occurs entirely in the cytoplasm, where single-stranded RNA forms a double-stranded (ds)-RNA intermediate, the main form of viral RNA genome inside the cell.

dsRNA produced during viral infection represents an important stimulus of the host innate immune response. It is recognized and engaged by three pattern recognition receptors. Toll-like receptor (TLR)-3 is localized to the endosomal and plasma membranes. TLR3 senses dsRNA released from dying cells and signals through its unique adaptor protein TIR-domain-containing adapter-inducing interferon-β (TRIF) (2). The cytoplasmic proteins retinoic acid-inducible gene (RIG)-I and melanoma differentiation-associated gene (MDA)-5 have recently been identified as intracellular receptors for viral dsRNA (3,4). RIG-I and MDA5 are homologous cytoplasmic helicases containing two amino-terminal caspase activation and recruitment domains (CARDS) and a carboxy-terminal DExD/H-Box RNA helicase domain. They bind to dsRNA through the helicase domain and signal through CARD domains to a common adaptor molecule, interferon-beta promoter stimulator (IPS)-1 (also called VISA) (5,6). Engagement of TLR3, RIG-I or MDA5 initiates signaling through two protein kinase complexes, TANK-binding kinase (TBK1)/IκB kinase-ε (IKKε) and IKKα/IKKβ, leading to activation of interferon regulated factor (IRF)-3 and nuclear factor (NF)-κB, respectively (7). Transcription factor activation, in turn, induces expression of IFNs and pro-inflammatory cytokines.

Although all three receptors can recognize viral dsRNA, they appear to be specialized in their recognition of particular viruses. RIG-I and TLR3 are required for respiratory syncytial virus (RSV)-induced expression of IFN-β, IP-10 in airway epithelial cells (8). RIG-I-deficient mice fail to produce type I IFNs in response to the negative-sense single-stranded RNA (ssRNA) viruses Newcastle disease virus, Sendai virus, vesicular stomatitis virus and influenza virus, and to the positive-sense ssRNA Japanese encephalitis virus, whereas MDA5-deficient mice fail to detect encephalomyocarditis (EMCV), a positive-sense ssRNA picornavirus (9). The engagement of PRRs is also cell-type specific: for example, while MDA5 is essential for induction of type I IFNs after infection with EMCV in fibroblasts and conventional dendritic cells (DCs), plasmacytoid DC use the TLR system for viral detection (9).

Little is known about the contributions of the various pattern recognition receptors to RV-induced responses in bronchial epithelial cells. Primary human bronchial epithelial cells express TLR3, and the TLR3 ligand polyI:C elicits a strong pro-inflammatory response in these cells (10,11). In 16HBE14o- human bronchial epithelial cells, TLR3 is primarily localized in the endosomes, not cell surface (12). TLR3 is partially required for RV39-induced IL-8 expression in 16HBE14o- cells (12) and RV1A-induced MUC5AC expression in NCI-H292 mucoepidermoid carcinoma cells (13). However, the requirement of either RIG-I or MDA5 for RV-induced responses has not yet been tested. In the present study, we found that MDA5 and TLR3, but not RIG-I, are required for RV-induced IFN responses in human airway epithelial cells.

Methods

Cell culture

BEAS-2B human bronchial epithelial cells, a SV-40-transformed airway bronchial epithelial cell line, were purchased from ATCC (Manassas, VA). Cells were grown on collagen-coated (5 μg/cm^2) plates in Bronchial Epithelial Growth Medium (BEGM, Lonza, Conshohocken, PA) containing epidermal growth factor (25 ng/ml), bovine pituitary extract (65 ng/ml), all-*trans* retinoic acid (5×10^{-8} M), hydrocortisone (0.5 μg/ml), insulin (5 μg/ml), transferrin (10

μg/ml), epinephrine (0.5μg/ml), triiodothyronine (6.5 ng/ml), gentamycin (50 μg/ml) and amphotericin (50 μg/ml).

Primary tracheal epithelial cells were all isolated from the tracheas of lung transplant donors, as described (14,15). Submerged cells were grown as monolayers to 80–100% confluence in BEGM containing epidermal growth factor (25 ng/ml), bovine pituitary extract (130 ng/ml), all-trans retinoic acid (5×10^{-8}M) and bovine serum albumin (1.5 μg/ml).

RV infection

RV1B and RV39 were obtained from ATTC. Viral stocks were generated by incubating HeLa cells with RV in serum-free medium until 80% of the cells were cytopathic. Viral stocks were concentrated, partially purified and titered as previously described (14,15). RV1B was irradiated with UV light at 100 μJ/cm^2 for 10 min on ice, using a CL-1000 crosslinker (UVP, Upland, CA).

Quantitative real-time PCR

Total RNA was extracted using the RNeasy kit (Qiagen, Valencia, CA), then transcibed to first-strand cDNA using Taqman Reverse Transcription Reagents (Applied Biosystems, Foster City, CA). First-strand cDNA is then used to quantify the expression of IFN-α, IFN-β, IFN-λ1, λ2/3, IRF-7, IP-10/CXCL-10, IL-8/CXCL8 and GM-CSF mRNA levels by quantitative real-time PCR (qPCR) using specific primers and probes.

Measurement of cytokine protein levels

BEAS-2B cells were grown to 80% confluence and infected with RV1B or medium alone for 1 h. Inoculum was then replaced BEGM. Twenty-four h later, supernatant was collected for the measurement of IFN-λ1, IP-10/CXCL-10 and IL-8/CXCL-8 protein by enzyme-linked immunosorbent assay (ELISA, R&D Systems, Minneapolis, MN).

Immunoblotting

Cells were lysed with RIPA buffer (50 mM Tris, pH7.4; 150 mM NaCl; 5 mM EDTA; 50 mM NaF; 1% NP-40; 10% glycerol). 30 μg of protein lysate was loaded in each well. Lysates were resolved by SDS-PAGE. Proteins were transferred to nitrocellulose or PVDF membrane. Membranes were blocked in 5% milk for 1 h at room temperature and probed with either mouse anti-RIG-I (Alexis Biochemicals, Plymouth Meeting, PA), goat anti-MDA5 (Santa Cruz Biotechnology, Santa Cruz, CA), rabbit anti-IRF3 (IBL America, Minneapolis, MN), rabbit anti-TRIF (Cell Signaling, Danvers, MA) or rabbit anti-IRF7 (Abcam, Cambridge, MA). Antibody binding was detected with a peroxidase-conjugated anti-mouse, anti-rabbit or anti-goat IgG and chemiluminescence.

Native PAGE to determine IRF3 dimerization

BEAS-2B cells were lysed with native PAGE sample prep kit (Invitrogen, Carlsbad, CA). Native PAGE was performed using 10% Ready Gel (Bio-rad, Hercules, CA), as described (16). The gel was pre-run with 25 mM Tris and 192 mM glycine, pH 8.4, with and without 1% deoxycholate in the cathode and anode chamber, respectively, for 30 min at 40 mA. Samples in the native sample buffer (10 μg protein, 62.5mM Tris-Cl, pH 6.8, and 15% glycerol) were applied to the gel and electrophoresed for 60min at 25 mA. Immunoblotting of IRF3 was performed as described above.

siRNA knockdown of RIG-I, MDA5, IRF3 and TRIF

19-bp duplex of targeting siRNA or non-targeting siRNA (Dharmacon, Lafayette, CO) was transfected into subconfluent BEAS-2B cells while cell seeding using RNAiMAX in OptiMEM (Invitrogen, Carlsbad, CA). A pool of double-stranded siRNAs containing equal parts of the following antisense sequences was used to knockdown RIG-I: 1, 5'-GCACAGAAGUGUAUAUUGG-3'; 2, 5'- CCACAACACUAGUAAACAA-3'; 3, 5'-CGGAUUAGCGACAAAUUUA-3'; 4, 5'-UCGAUGAGAUUGAGCAAGA-3'. The non-targeting siRNA sequence was 5'-CGAACUCACUGGUCUGACCdtdt-3'(sense), 5'-GGUCAGACCAGUGAGUUCG-dtdt-3'(antisense). For knockdown of MDA5, a pool of the following sequences was used: 1, 5'-GAAUAACCCAUCACUAAUA -3'; 2, 5'-GCACGAGGAAUAAUCUUUA -3'; 3, 5'-UGACACAAUUCGAAUGAUA -3'; 4, 5'-CAAUGAGGCCCUACAAAUU'-3'. For knockdown of IRF3, a pool of the following sequences was used: 1, 5'-CGAGGCCACUGGUGCAUAU-3'; 2, 5'-CCAGACACCUCUCCGGACA-3'; 3, 5'-GGAGUGAUGAGCUACGUGA-3', 4, 5'-AGACAUUCUGGAUGAGUUA-3'. For knockdown of TRIF, a pool of the following sequences was used: 1, 5'-GGAGCCACAUGUCAUUUGG-3'; 2, 5'-CCAUAGACCACUCAGCUUU-3'; 3, 5'-GGACGAACACUCCCAGAUC-3'; 4, 5'-CCACUGGCCUCCCUGAUAC-3'. The next morning, cells were incubated in fresh BEGM containing for 24 h. Finally, cells were treated with the relevant stimulus in BEGM medium for one day prior to harvest.

Data analysis

SigmaStat computing software (SPSS, Chicago, IL) was used for data analysis. Data are represented as mean±SEM. Normality was tested using the Kolmogorov-Smirnov test. Statistical significance was assessed by either one-way analysis of variance (ANOVA) or the Kruskal-Wallis one-way ANOVA based on ranks, whenever appropriate. Differences identified by ANOVA were pinpointed by the Student Newman-Keuls' multiple range test.

Results

RV1B-induced IFN expression in BEAS-2B human bronchial epithelial cells

To test whether RV induces an IFN response in human bronchial epithelial cells, BEAS-2B cells were infected with intact RV1B or UV-irradiated RV-1B for 1 h at 33°C. Cellular total RNA was extracted from lysates to measure the gene expression at 1, 8, 18, 24, 48 and 72 h post-infection by quantitative PCR. Compared with replication-deficient UV-irradiated virus, intact RV1B increased the mRNA expression of IFN-β, IFN-λ1 and IFN-λ2/3, as well as the expression of several interferon-stimulated genes (ISGs) including IRF7, RIG-I, MDA5 and TLR3 (Figure 1). The peak level of mRNA expression was 24 h post-infection, except in the case of IFN-β, which was 48 h post-infection. The fold-induction varied widely, from 4-fold (TLR3) to approximately 27,000-fold (IFN-λ2/3). Fold-increases in IFN and ISG mRNA expression tended to be higher for genes expressed at lower levels as baseline, as measured by cycle number (Table 1). RV1B infection also increased the protein expression of IFN-λ1, IP-10/CXCL-10 and IL-8/CXCL-8 (Figure 2A–C). However, there was no induction of IRF7 protein expression (Figure 2D). Nevertheless, these data, combined with increases in RIG-I and MDA5 protein abundance (see below), demonstrate that RV induces a robust, replication-dependent innate immune response at both the mRNA and protein levels. RV1B infection also increased IFN and ISG mRNA expression in primary tracheal epithelial cells (Figure 3, Table 2).

MDA5 and TLR3, but not RIG-I, are required for RV-induced innate immune responses

Viral dsRNA generated during replication may be detected by the PRRs, RIG-I, MDA5 and/or TLR3. To determine which PRR is responsible for sensing RV dsRNA and inducing the innate immune response, we employed siRNA against RIG-I, MDA5 and the TLR3 adaptor protein TRIF/TICAM. Forty-eight h later, cells were infected with RV1B, UV-irradiated RV-1B or sham HeLa cell lysate, and the expression of IFNs and ISGs was measured by qPCR 24 h after infection. RIG-I expression was knocked down by 80–90% following treatment with RIG-I siRNA (Figure 4A). Immunoblots also showed a significant increase in RIG-I protein expression with RV1B treatment, suggesting that expression of RIG-I is inducible. RIG-I siRNA had a slight inhibitory effect on the expression of its homologue protein, MDA5 (Figure 4B). However, RIG-I siRNA failed to decrease RV-induced expression of IFNs or ISGs compared to non-targeting siRNA, suggesting that RIG-I is not required for sensing RV dsRNA (Figure 5).

Next, we knocked down MDA5 expression using MDA5 siRNA (Figure 4C). Again, an 80–90% knockdown efficiency was achieved. MDA5 protein expression was also induced by RV1B infection. MDA5 siRNA had no effect on RIG-I protein expression (Figure 4D). After transfection with MDA5 siRNA, there was a significant decrease in expression of RV1B-induced IFN-β, -λ1 and -λ2/3 compared to cells transfected with non-targeting siRNA (Figure 6). MDA5 siRNA also decreased RV1B-induced mRNA expression of the ISGs IRF7 and IP-10/CXCL10. Unlike IFNs, MDA5 siRNA treatment was associated with a paradoxic increase in RV1B-induced expression of IL-8 and GM-CSF. Together, these data suggest that MDA5, but not RIG-I, is required for maximal RV-induced IFN responses, but not for RV-induced cytokine responses.

To examine whether MDA-5 is also required for major group RV-induced IFN responses, we repeated our experiment using RV39. BEAS-2B cells were transfected with either MDA5 or non-targeting siRNA and then infected with RV39, UV-irradiated RV39 or sham HeLa cell lysate. Twenty-four h after infection, cellular RNA was extracted to measure the expression of IFNs and ISGs by quantitative PCR (Figure 7). There was a significant decrease in mRNA expression of IFN-β, -λ1 and -λ2/3 in cells transfected with MDA5 siRNA compared to cells transfected with non-targeting siRNA. MDA5 siRNA also decreased RV39-induced mRNA expression of the ISGs, IRF7 and IP-10/CXCL10.

We then sought to determine whether MDA-5 is required for the recognition of viral dsRNA in primary tracheal epithelial cells as in BEAS-2B cells. Primary cells were cultured until 70% confluent and then transfected with siRNA against MDA5 or non-targeting siRNA. Forty-eight h later, cells were infected with RV1B or UV-irradiated RV1B. Cellular mRNA was extracted 24 h after infection to determine mRNA expression by qPCR. Compared to non-targeting siRNA, MDA5 siRNA decreased RV1B-induced expression of IFN-β, IFN-λ_1, IFN-$\lambda_{2/3}$, IRF7 and IP-10/CXCL10 (Figure 8). These data confirm that MDA5 is required for sensing RV dsRNA and induction of the subsequent IFN response in primary cells.

Next. we blocked TLR3 signaling using siRNA against TRIF/TICAM, the TLR3 adaptor molecule. Again, a high knockdown efficiency was verified by immunoblotting (Figure 9). Like MDA5 siRNA, TRIF siRNA abolished RV-1B induced expression of IFN-β, IFN-λ_1, IFN-$\lambda_{2/3}$, IRF7 and IP-10/CXCL10, suggesting TLR3 signaling is also required for maximal RV1B-induced IFN responses.

IRF3 is required for RV1B-induced IFN responses

IRF3 is a ubiquitously-expressed transcription factor which regulates type I IFN production. To test whether RV1B induces IRF3 activation, BEAS-2B cells were infected with RV1B or UV-irradiated RV-1B. Cell protein lysates were collected 12 h after infection. IRF3

phosphorylation shift was determined by SDS-PAGE followed by immunoblotting using anti-IRF3 antibody (Figures 10A, 10B), and IRF3 dimerization determined by native PAGE (Figure 10C). PolyI:C, a synthetic dsRNA which induced both IRF3 phosphorylation and dimerization, served as a positive control. We found that RV1B, but not UV-irradiated RV-1B, induced IRF3 phosphorylation and dimerization. Similar results were observed in primary tracheal epithelial cells (Figure 10D).

We then examined the requirement of IRF3 in RV-induced IFN responses using siRNA against IRF3. IRF3 protein abundance was substantially knocked down by IRF3 siRNA (Figure 11). IRF3 siRNA nearly abolished RV-1B-induced expression of IFNs β, λ 1 and λ2/3, IRF7 and IP-10/CXCL10. However, there was no effect on IL-8 or GM-CSF expression. Taken together, these data suggests that IRF3 is activated by RV1B, and that IRF3 is required for RV-induced IFN responses, as well as the expression of ISGs such as IRF7 and IP-10.

IRF3 functions downstream of MDA5 signaling

RIG-I/MDA5 and TLR3 signaling pathways converge on a common TRAF3 (TNF receptor associated factor 3) adapter complex, which then activates two IRF3 kinases, TBK1 and IKK-ε (7). To examine whether IRF3 functions downstream of MDA5 in airway epithelial cells, BEAS-2B cells were transfected with either MDA5 siRNA or non-targeting siRNA, then infected with RV-1B, UV-irradiated RV-1B or sham HeLa cell lysate. IRF3 dimerization was resolved by native PAGE (Figure 12). We found that MDA5 and TRIF siRNA each caused a partial reduction in RV-induced IRF3 dimerization compared to non-targeting siRNA-transfected cells, confirming in airway epithelial cells the general notion that IRF3 functions downstream of MDA5 and TRIF.

Discussion

Host pathogen recognition, as reflected by the induction of type I interferons is mediated by activation of pattern recognition receptors. The membrane dsRNA receptor, TLR3, and the recently-identified cytoplasmic dsRNA receptors, RIG-I and MDA5, are responsible for sensing viral dsRNA (2–4). Although all three receptors can recognize viral dsRNA, the engagement of receptor and viral dsRNA seem to be cell type and virus-specific. RIG-I-deficient mice fail to produce type I IFNs in response to the negative-sense single-stranded RNA (ssRNA) viruses Newcastle disease virus, Sendai virus, vesicular stomatitis virus and influenza virus, and to the positive-sense ssRNA Japanese encephalitis virus, whereas MDA5-deficient mice fail to detect EMCV, a positive-sense ssRNA picornavirus (9). Whereas MDA5 is essential for induction of type I IFNs after infection with EMCV in fibroblasts and conventional dendritic cells, plasmacytoid DC use the TLR system for viral detection (9). While these results are compelling, it seems premature to conclude that all picornaviruses are sensed by MDA5 in all cell types, because only cardioviruses have been studied.

In this manuscript, we found that infection of BEAS-2B and primary tracheal epithelial cells with RV induced substantial increases in IFN and ISG mRNA expression. In limited studies, we also found similar changes in gene expression following infection with major and minor group virus. Due to the low level of baseline IFN expression, the fold-increases in IFN expression were quite high, perhaps artificially so. However, increases in IFN-λ1, IP-10/CXCL-10, RIG-I and MDA-5 were verified by ELISA and immunoblotting, implying that RV significantly increases IFN responses in airway epithelial cells. Further, we demonstrate for the first time that MDA5 and TRIF, but not RIG-I, are required for maximal sensing RV dsRNA in human airway epithelial cells. Transfection of both a human bronchial epithelial cell line (BEAS-2B cells) and primary tracheobronchial epithelial cells with siRNA against

MDA5, but not non-targeting siRNA, significantly inhibited RV1B-induced expression of a type I IFN, IFN-β, as well as a number of ISGs. Knockdown of MDA5 also attenuated expression of the type III IFNs IFN-λ1 and -λ2/3, which functionally resemble type I IFNs (17) and are also induced by RV infection (18). These data are in agreement with previous data suggesting MDA5 is required for sensing picornavirus dsRNA (9). On the other hand, our data contrast with previous data from A549 alveolar type II epithelial cells showing that RIG-I and TLR3, but not MDA5, are required for sensing human RSV, a paramyxovirus (8). Thus, in the airway epithelium, recognition of viral dsRNA is indeed virus type-specific.

We also examined the contribution of IRF3 to RV-induced responses in airway epithelial cells. IRF3 siRNA nearly abolished IFN and ISG expression. MDA5 and TRIF knockdown also decreased IRF3 dimerization. These data are consistent with the idea that TLR3 and MDA5 regulate IFN expression via a common downstream intermediate, IRF3.

In contrast to siRNA against MDA5, siRNA against RIG-I had no effect on RV-induced IRF3 dimerization or IFN expression. The divergent roles of RIG-I and MDA5 in the context of RV infection suggest that the two homologous helicases function distinctly from each other. Further, though RIG-I expression was induced after RV infection, RIG-I apparently cannot compensate for reduced expression and/or function of MDA5.

Using siRNA against MDA5 and IRF3, we found that MDA5/IRF3 signaling is required for RV-induced IFN, but not IL-8 expression. Indeed, expression of IL-8 and GM-CSF were often paradoxically increased. Previous studies have shown that RV-induced IL-8 expression is strictly regulated by the transcription factor NF-κB (14,19). The initial phase of IL-8 expression is also replication-independent (14,20–22). Inhibition of dsRNA sensing would therefore not be expected to reduce IL-8 expression. Further, the upregulation of pro-inflammatory cytokine expression following MDA5 and IRF3 knockdown may represent a compensatory mechanism by which the airway epithelial cells increase immune surveillance when the IFN response is suppressed.

We previously showed that TLR3 was partially required for RV39-induced IL-8 expression in 16HBE14o- cells (12). In the present study, we could not verify TLR3 knockdown by immunoblotting or flow cytometry in BEAS-2B cells (not shown), leading us to employ siRNA against TRIF. In contrast to MDA-5 knockdown, inhibition of TLR3 signaling using TRIF siRNA inhibited both IFN and IL-8 expression. Based on our previous result, the complete effect of TRIF siRNA on IFN signaling was unexpected, consistent with the notion that other, as yet unknown pattern recognition receptors utilize TRIF as an adaptor. In any event, the differential effects of MDA-5 and TRIF siRNA on IL-8 expression suggest that, although NF-κB and IRF3 are both components of the same transcriptional enhanceosome in the regulation of IFNs, ISGs and inflammatory cytokine IL-8 (23,24), their requirement for gene expression may vary for different target genes, perhaps depending on the organization of IFN-stimulated and NF-κB response elements in the promoter.

It has recently been reported that picornaviruses may develop strategies to escape host immune surveillance. Hepatitis A virus has been shown to suppress RIG-I-mediated signaling in fetal rhesus monkey kidney (FRhK-4) cells (25). Poliovirus infection induces cleavage of MDA5 in HeLa cells (26). In A549 human alveolar type II alveolar epithelial cells, RV14 infection fails to induce high levels of IFN, apparently by interfering with IRF3 dimerization (27). In this study, RV1B induced robust IRF3 dimerization and IFN responses in both BEAS-2B and primary bronchial epithelial cells. Also, while we did indeed observe apparent degradation of MDA5 following viral infection (Figure.5), the total protein abundance of MDA5 was still substantially increased 24 h after RV inoculation. Taken together, these data suggest an intact host innate immune defense against RV1B dsRNA.

We confined most of our studies of RV-induced IFN responses to the minor group serotype RV1B. However, IFN expression by RV39, a major group virus, was also blocked by MDA-5 but not RIG-I siRNA. This was not unexpected, as RV1B and RV16, another major group serotype, have been shown to induce nearly identical patterns of gene expression in primary cultured airway epithelial cells (28). We have found that infection with RV1B and RV39 induce similar levels of Akt phosphorylation and IL-8 expression in cultured 16HBE14o-human bronchial epithelial cells, and that inhibition of PI 3-kinase blocks both RV1B- and RV39-induced IL-8 expression induced by either virus (29). Thus, there are ample data suggesting that major and minor subgroup RV stimulate similar airway epithelial cell signaling pathways and elicit similar immune responses.

In conclusion, we have shown for the first time that MDA5, TLR3 and IRF3 are each required for maximal RV-induced IFN responses. Viral infections, most commonly caused by RV, are the most frequent cause of asthma exacerbations, and account for a substantial percentage of chronic obstructive pulmonary disease exacerbations (1). Bronchial epithelial cells isolated from patients with asthma have been demonstrated to have an incomplete innate immune response to rhinovirus infection, with deficient type I IFN-β and type III IFN-λ production (18,30). Further understanding of the biochemical signaling pathways regulating RV-induced IFN expression may therefore provide insight into the pathogenesis of human airway diseases and new therapeutic targets for treatment.

Acknowledgments

The authors thank Drs. Nathalie Grandvaux and John Hiscott, McGill University, for their advice in the measurement of IRF3 dimerization.

This work was supported by National Institutes of Health grants HL81420 and 82550 (M.B.H.)

References

1. Hershenson MB, Johnston SL. Rhinovirus infections: More than a common cold. Am. J. Respir. Crit. Care Med 2006;174:1284–1285. [PubMed: 17158286]
2. Yamamoto M, Sato S, Hemmi H, Hoshino K, Kaisho T, Sanjo H, Takeuchi O, Sugiyama M, Okabe M, Takeda K, Akira S. Role of adaptor TRIF in the MyD88-independent Toll-like receptor signaling pathway. Science 2003;301:640–643. [PubMed: 12855817]
3. Yoneyama M, Kikuchi M, Natsukawa T, Shinobu N, Imaizumi T, Miyagishi M, Taira K, Akira S, Fujita T. The RNA helicase RIG-I has an essential function in double-stranded RNA-induced innate antiviral responses. Nat. Immunol 2004;5:730–737. [PubMed: 15208624]
4. Andrejeva J, Childs KS, Young DF, Carlos TS, Stock N, Goodbourn S, Randall RE. The V proteins of paramyxoviruses bind the IFN-inducible RNA helicase, MDA-5, and inhibit its activation of the IFN-b promoter. Proc. Natl. Acad. Sci. USA 2004;101:17264–17269. [PubMed: 15563593]
5. Kawai T, Takahashi K, Sato S, Coban C, Kumar H, Kato H, Ishii KJ, Takeuchi O, Akira S. IPS-1, an adaptor triggering RIG-I- and MDA5-mediated type I interferon induction. Nat. Immunol 2005;6:981–988. [PubMed: 16127453]
6. Xu L-G, Wang Y-Y, Han K-J, Li L-Y, Zhai Z, Shu H-B. VISA is an adapter protein required for virus-triggered IFN-b signaling. Molecular Cell 2005;19:727–740. [PubMed: 16153868]
7. Fitzgerald KA, McWhirter SM, Faia KL, Rowe DC, Latz E, Golenbock DT, Coyle AJ, Liao SM, Maniatis T. IKKepsilon and TBK1 are essential components of the IRF3 signaling pathway. Nat. Immunol 2003;4:491–496. [PubMed: 12692549]
8. Liu P, Jamaluddin M, Li K, Garofalo RP, Casola A, Brasier AR. Retinoic acid inducible gene-I mediates early anti-viral response and Toll like receptor 3 expression in respiratory syncytial virus - infected airway epithelial cells. J Virol 2007;81:1401–1411. [PubMed: 17108032]
9. Kato H, Takeuchi O, Sato S, Yoneyama M, Yamamoto M, Matsui K, Uematsu S, Jung A, Kawai T, Ishii KJ, Yamaguchi O, Otsu K, Tsujimura T, Koh CS, Reis e Sousa C, Matsuura Y, Fujita T, Akira

S. Differential roles of MDA5 and RIG-I helicases in the recognition of RNA viruses. Nature 2006;441:101–105. [PubMed: 16625202]

10. Muir A, Soong G, Sokol S, Reddy B, Gomez MI, van Heeckeren A, Prince A. Toll-like receptors in normal and cystic fibrosis airway epithelial cells. Am. J. Respir. Cell Mol. Biol 2004;30:777–783. [PubMed: 14656745]
11. Sha Q, Truong-Tran AQ, Plitt JR, Beck LA, Schleimer RP. Activation of airway epithelial cells by Toll-like receptor agonists. Am. J. Respir. Cell Mol. Biol 2004;31:358–364. [PubMed: 15191912]
12. Sajjan US, Jia Y, Newcomb DC, Bentley JK, Lukacs NW, LiPuma JJ, Hershenson MB. H. influenzae potentiates airway epithelial cell responses to rhinovirus by increasing ICAM-1 and TLR3 expression. FASEB J 2006;20:2121–2123. [PubMed: 16914605]
13. Zhu L, Lee P-k, Lee W-M, Zhao Y, Yu D, Chen Y. Rhinovirus induced major airway mucin production involves a novel TLR3-EGFR dependent pathway. Am. J. Respir. Cell Mol. Biol 2009;40:610–619. [PubMed: 18978302]
14. Newcomb DC, Sajjan U, Nanua S, Jia Y, Goldsmith AM, Bentley JK, Hershenson MB. Phosphatidylinositol 3-kinase is required for rhinovirus-induced airway epithelial cell interleukin-8 expression. J. Biol. Chem 2005;280:36952–36961. [PubMed: 16120607]
15. Papi A, Johnston SL. Rhinovirus infection induces expression of its own receptor intercellular adhesion molecule 1 via increased NF-kappaB-mediated transcription. J. Biol. Chem 1999;274:9707–9720. [PubMed: 10092659]
16. Iwamura T, Yoneyama M, Yamaguchi K, Suhara W, Mori W, Shiota K, Okabe Y, Namiki H, Fujita T. Induction of IRF-3/-7 kinase and NF-kB in response to double-stranded RNA and virus infection: common and unique pathways. Genes to Cells 2001;6:375–388. [PubMed: 11318879]
17. Kotenko SV, Gallagher G, Baurin VV, Lewis-Antes A, Shen M, Shah NK, Langer JA, Sheikh F, Dickensheets H, Donnelly RP. IFN-lambdas mediate antiviral protection through a distinct class II cytokine receptor complex. Nat. Immunol 2003;4:69–77. [PubMed: 12483210]
18. Contoli M, Message SD, Laza-Stanca V, Edwards MR, Wark PA, Bartlett NW, Kebadze T, Mallia P, Stanciu LA, Parker HL, Slater L, Lewis-Antes A, Kon OM, Holgate ST, Davies DE, Kotenko SV, Papi A, Johnston SL. Role of deficient type III interferon-lambda production in asthma exacerbations. Nat. Med 2006;12:1023–1026. [PubMed: 16906156]
19. Zhu Z, Tang W, Gwaltney JM, Wu Y, Elias JA. Rhinovirus stimulation of interleukin-8 in vivo and in vitro: role of NF-kappaB. Am. J. Physiol. Lung Cell. Mol. Physiol 1997;273:L814–L824.
20. Griego SD, Weston CB, Adams JL, Tal-Singer R, Dillon SB. Role of p38 mitogen-activated protein kinase in rhinovirus-induced cytokine production by bronchial epithelial cells. J. Immunol 2000;165:5211–5220. [PubMed: 11046054]
21. Suzuki T, Yamaya M, Sekizawa K, Hosoda M, Yamada N, Ishizuka S, Nakayama K, Yanai M, Numazaki Y, Sasaki H. Bafilomycin A(1) inhibits rhinovirus infection in human airway epithelium: effects on endosome and ICAM-1. Am. J. Physiol. Lung Cell. Mol. Physiol 2001;280:L1115–L1127. [PubMed: 11350790]
22. Kaul P, Biagioli MC, Singh I, Turner RB. Rhinovirus-induced oxidative stress and interleukin-8 elaboration involves p47-phox but is independent of attachment to intercellular adhesion molecule-1 and viral replication. J. Infect. Dis 2000;181:1885–1890. [PubMed: 10837166]
23. Ohmori Y, Hamilton TA. Cooperative interaction between interferon (IFN) stimulus response element and kappa B sequence motifs controls IFN gamma- and lipopolysaccharide-stimulated transcription from the murine IP-10 promoter. J. Biol. Chem 1993;268:6677–6688. [PubMed: 8454640]
24. Casola A, Garofalo RP, Jamaluddin M, Vlahopoulos S, Brasier AR. Requirement of a novel upstream response element in respiratory syncytial virus-induced IL-8 gene expression. J. Immunol 2000;164:5944–5951. [PubMed: 10820277]
25. Fensterl V, Grotheer D, Berk I, Schlemminger S, Vallbracht A, Dotzauer A. Hepatitis A virus suppresses RIG-I-mediated IRF-3 activation to block induction of beta interferon. J. Virol 2005;79:10968–10977. [PubMed: 16103148]
26. Barral PM, Morrison JM, Drahos J, Gupta P, Sarkar D, Fisher PB, Racaniello VR. MDA-5 is cleaved in poliovirus-infected cells. J. Virol 2007;81:3677–3684. [PubMed: 17267501]

27. Kotla S, Peng T, Bumgarner RE, Gustin KE. Attenuation of the type I interferon response in cells infected with human rhinovirus. Virology 2008;374:399–410. [PubMed: 18272195]

28. Chen Y, Hamati E, Lee P-K, Lee W-M, Wachi S, Schnurr D, Yagi S, Dolganov G, Boushey H, Avila P, Wu R. Rhinovirus induces airway epithelial gene expression through double-stranded RNA and IFN-dependent pathways. Am. J. Respir. Cell Mol. Biol 2006;34:192–203. [PubMed: 16210696]

29. Newcomb DC, Sajjan US, Nagarkar DR, Wang Q, Nanua S, Zhou Y, McHenry CL, Hennrick KT, Tsai WC, Bentley JK, Lukacs NW, Johnston SL, Hershenson MB. Human rhinovirus 1B exposure induces phosphatidylinositol 3-kinase-dependent airway inflammation in mice. Am. J. Respir. Crit. Care Med 2008;177:1111–1121. [PubMed: 18276942]

30. Wark PAB, Johnston SL, Bucchieri F, Powell R, Puddicombe S, Laza-Stanca V, Holgate ST, Davies DE. Asthmatic bronchial epithelial cells have a deficient innate immune response to infection with rhinovirus. J. Exp. Med 2005;201:937–947. [PubMed: 15781584]

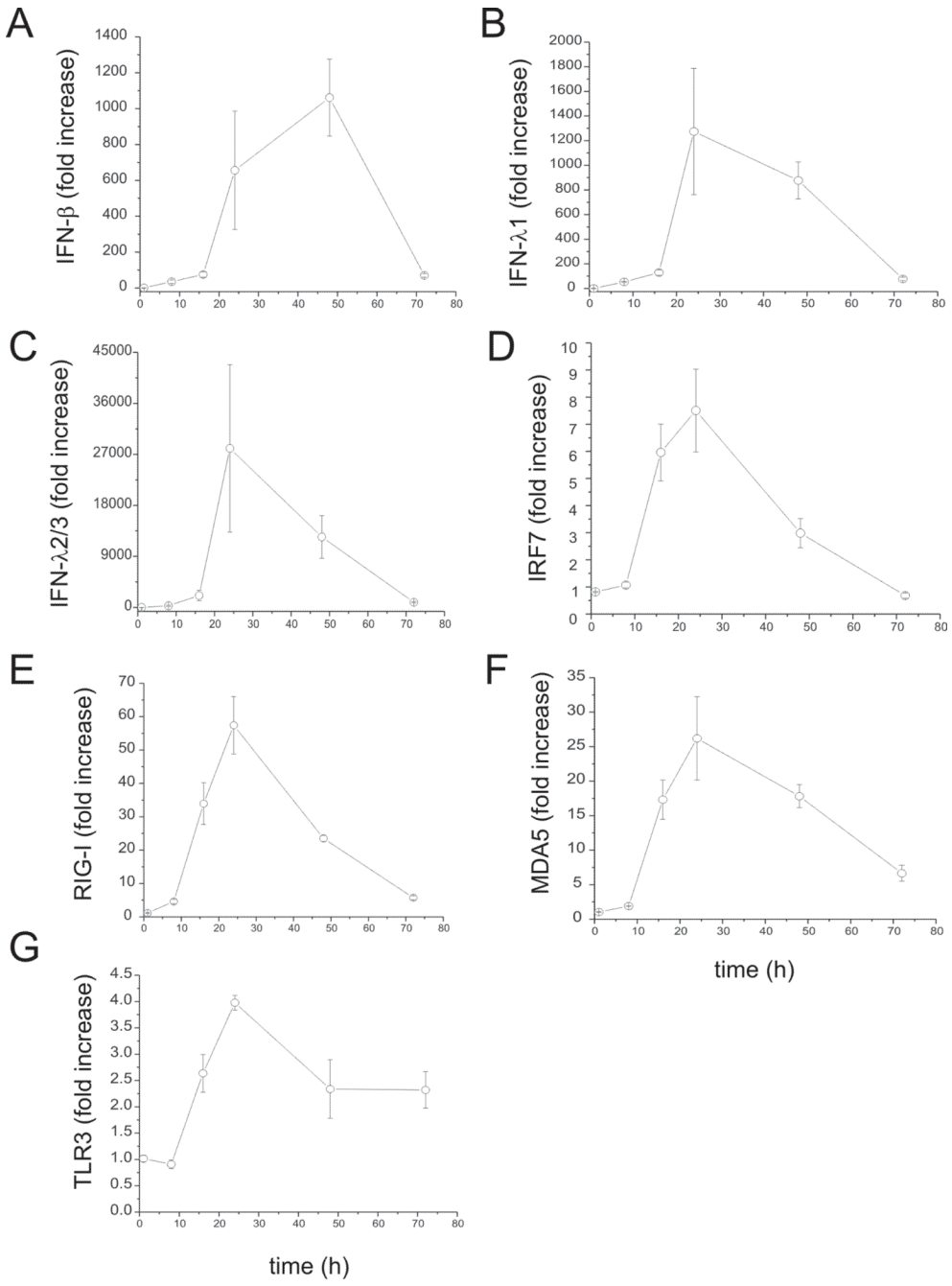

Figure 1. Fold increase of RV1B-induced IFN and ISG responses in cultured airway epithelial cells

BEAS-2B cells were infected with RV1B or sham (1 h at 33°C). Total RNA was extracted at 1, 8, 16, 24, 48 and 72 hours after infection. A–G. The expression of IFN-β, IFN-λ1, IFN-λ2/3, IRF7, RIG-I, MDA5 and TLR3 at each time point was determined by qPCR. The expression of each target gene was normalized to GAPDH. Expression levels are represented as the ratio of the response to intact RV vs. the response to sham. Data represent mean ± SEM for three experiments.

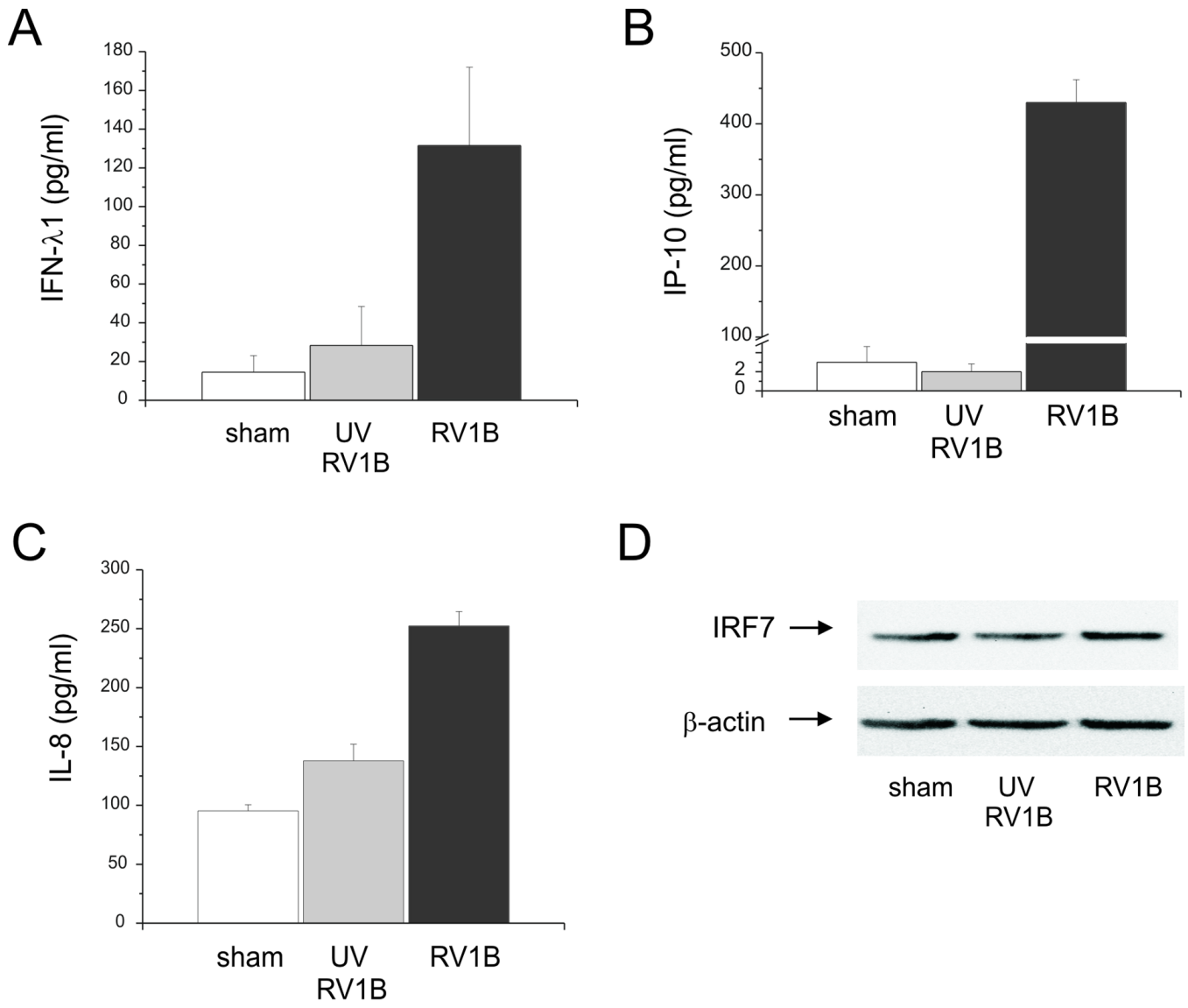

Figure 2.

RV1B-induced protein expression of IFNs and ISGs. BEAS-2B cells were grown to near confluence and infected with RV1B, UV-irradiated RV1B or sham. A–C. Medium supernatants were extracted twenty-four hours after infection for ELISA to determine the expression of IFN-λ1, IP-10 and IL-8. D. Protein lysates were used to determine IRF7 expression by immunoblotting.

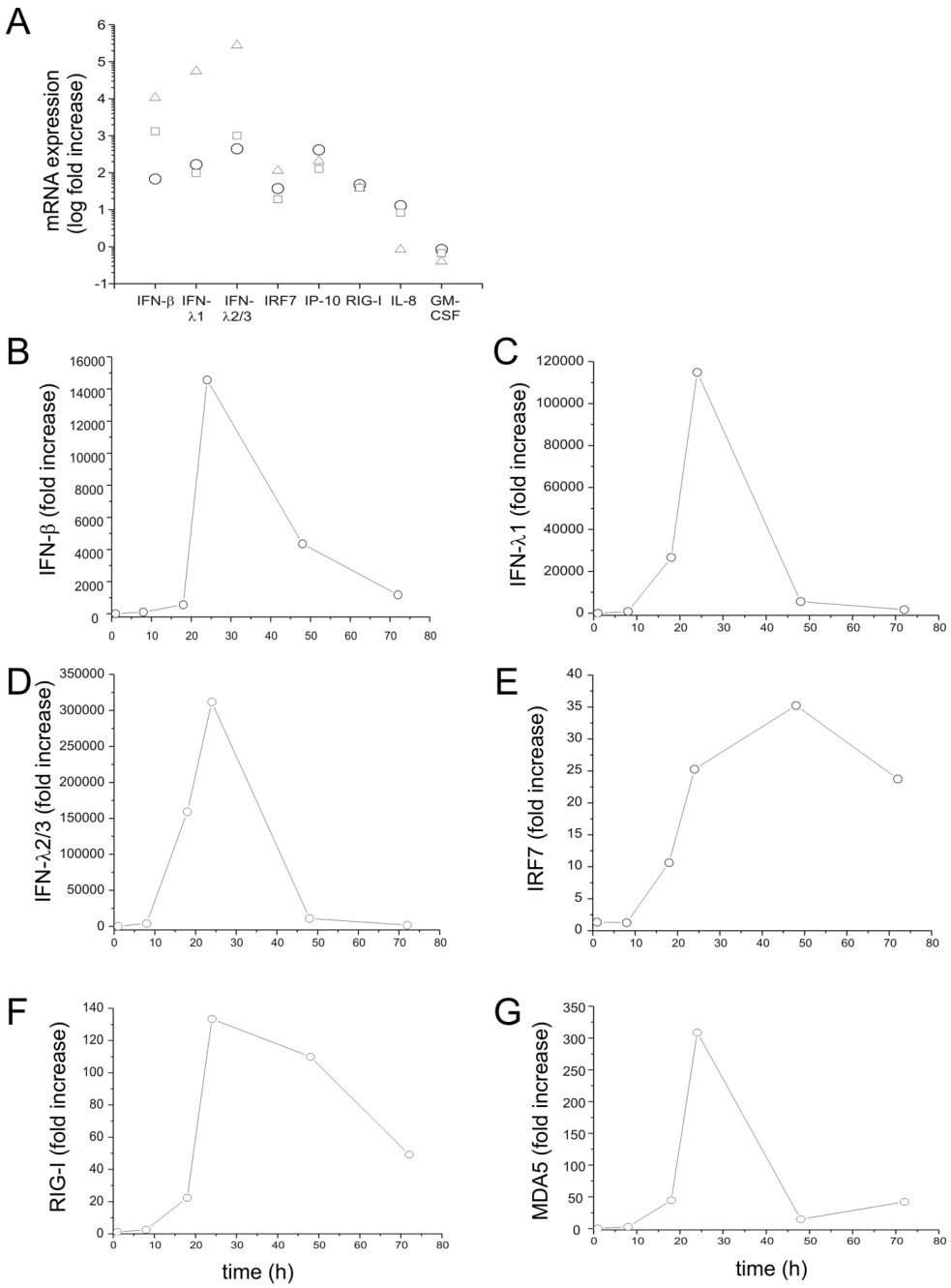

Figure 3. RV1B-induced expression of IFNs, ISGs and chemokines in primary tracheobronchial epithelial cells

Primary tracheobronchial epithelial cells were grown to near confluence and infected with RV1B or sham. A. Total RNA was extracted twenty-four hour after infection, and the expression of IFN-β, IFN-λ1, IFN-λ2/3, IRF7, IP-10, IL-8 and GM-CSF determined by qPCR. Expression levels are represented as the ratio of the response to intact RV vs. the response to sham. The y-axis is in log scale. B–G. Time course of RV1B-induced responses in primary cells.

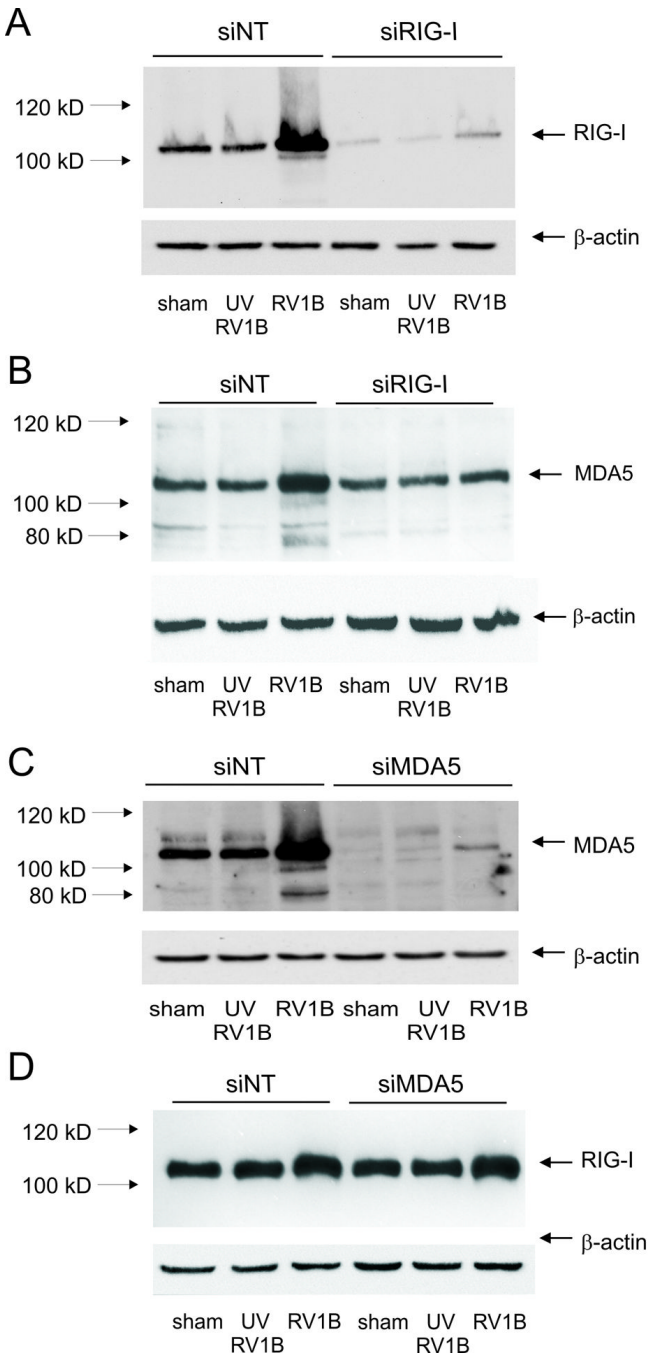

Figure 4. RIG-I and MDA-5 siRNA knockdown efficiencies

A, B. RIG-I or non-targeting siRNA was transfected into BEAS-2B cells. After transfection, cells were infected with RV1B, UV-irradiated RV1B (UV-RV1B) or sham. After infection, cell lysates were probed with antibodies against RIG-I (A) or MDA-5 (B). Note the inductions in RIG-I and MDA5 expression with intact RV, as well as the apparent degradation of MDA-5 following viral infection. C, D. MDA5 or non-targeting siRNA was transfected into BEAS-2B cells. After transfection, cells were infected with RV1B, UV-irradiated RV1B (UV-RV1B) or sham. After infection, cell lysates were probed with antibodies against either MDA5 (C) or RIG-I (D). (The blots shown are a representative of three separate experiments.)

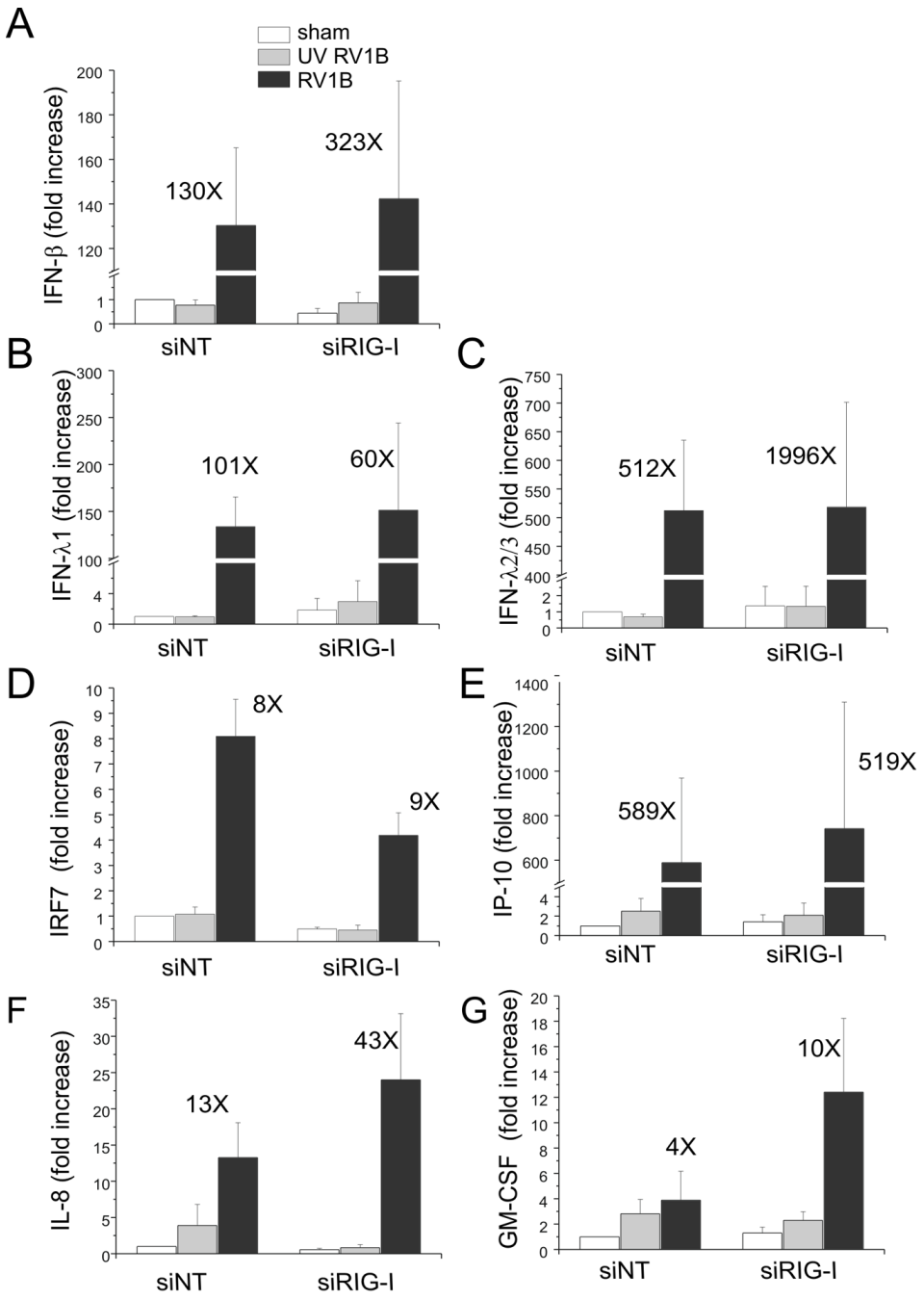

Figure 5. siRNA against RIG-I does not block RV1B-induced IFN and ISG expression

A–G. Total RNA was extracted and the expression of IFN-β, IFN-λ1, IFN-λ2/3, IRF7, IP-10, IL-8 and GM-CSF was determined by qPCR. The expression of each target gene was normalized to GAPDH. Expression levels are represented as the fold increase vs. sham-infected, non-targeting siRNA-transfected cells. The y-axis has been broken in order to show the effects of siRNA on both basal and maximal gene expression. Bars represent mean ± SEM for four experiments; numbers on top of bars indicate the fold increase compared to sham-infected sample within its own siRNA group. (*$p<0.05$ vs. RIG-I siRNA-transfected RV1B-infected sample, ANOVA.)

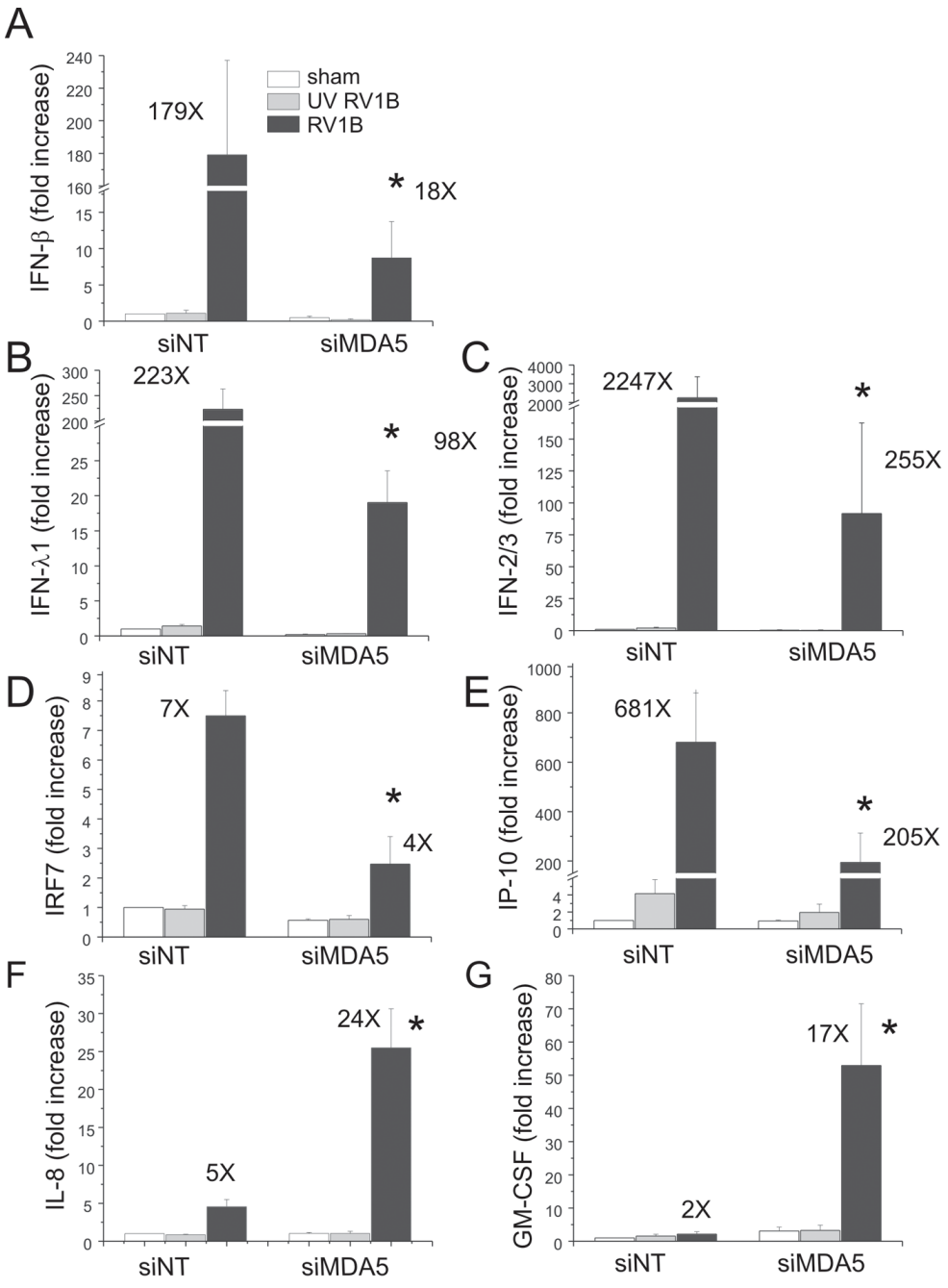

Figure 6. siRNA against MDA5 blocks RV1B-induced IFN and ISG expression

A–G. Total RNA was extracted and the expression of IFN-β, IFN-λ1, IFN-λ2/3, IRF7, IP-10, IL-8 and GM-CSF was determined by qPCR. The expression of each target gene was normalized to GAPDH. Expression levels are represented as the fold increase vs. sham-infected, non-targeting siRNA-transfected cells. The y-axis has been broken in order to show the effects of siRNA on both basal and maximal gene expression. Bars represent mean ± SEM for five experiments; numbers on top of bars indicate the fold increase compared to sham-infected sample within its own siRNA group. (*$p<0.05$ vs. MDA5 siRNA-transfected RV-infected sample, ANOVA.)

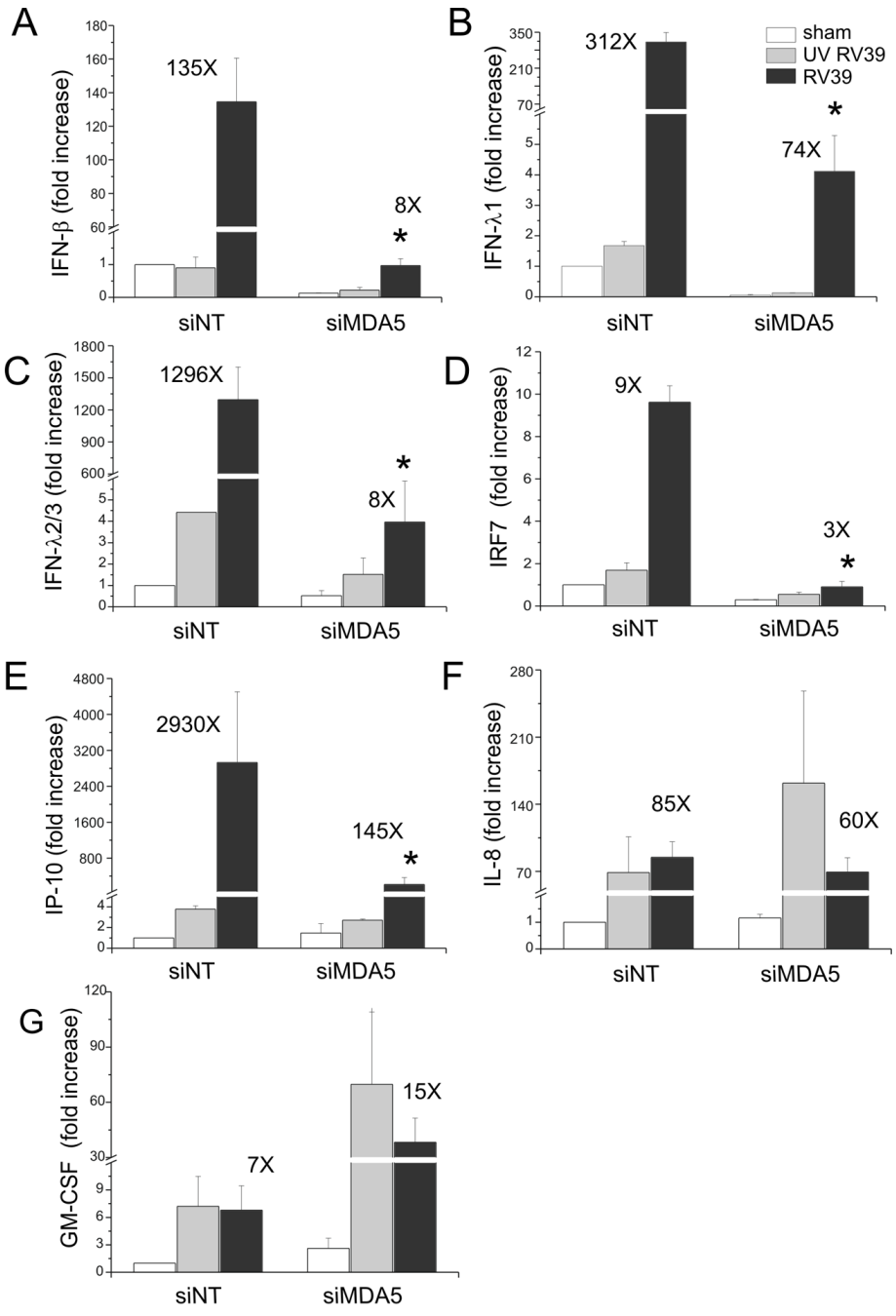

Figure 7. siRNA against MDA5 blocks RV39-induced IFN and ISG expression

A–G. Total RNA was extracted and the expression of IFN-β, IFN-λ1, IFN-λ2/3, IRF7, IP-10, IL-8 and GM-CSF was determined by qPCR. The expression of each target gene was normalized to GAPDH. Expression levels are represented as the fold increase vs. sham-infected, non-targeting siRNA-transfected cells. The y-axis has been broken in order to show the effects of siRNA on both basal and maximal gene expression. Bars represent mean ± SEM for three experiments; numbers on top of bars indicate the fold increase compared to sham-infected sample within its own siRNA group. (*$p<0.05$ vs. MDA5 siRNA-transfected RV-infected sample, ANOVA.)

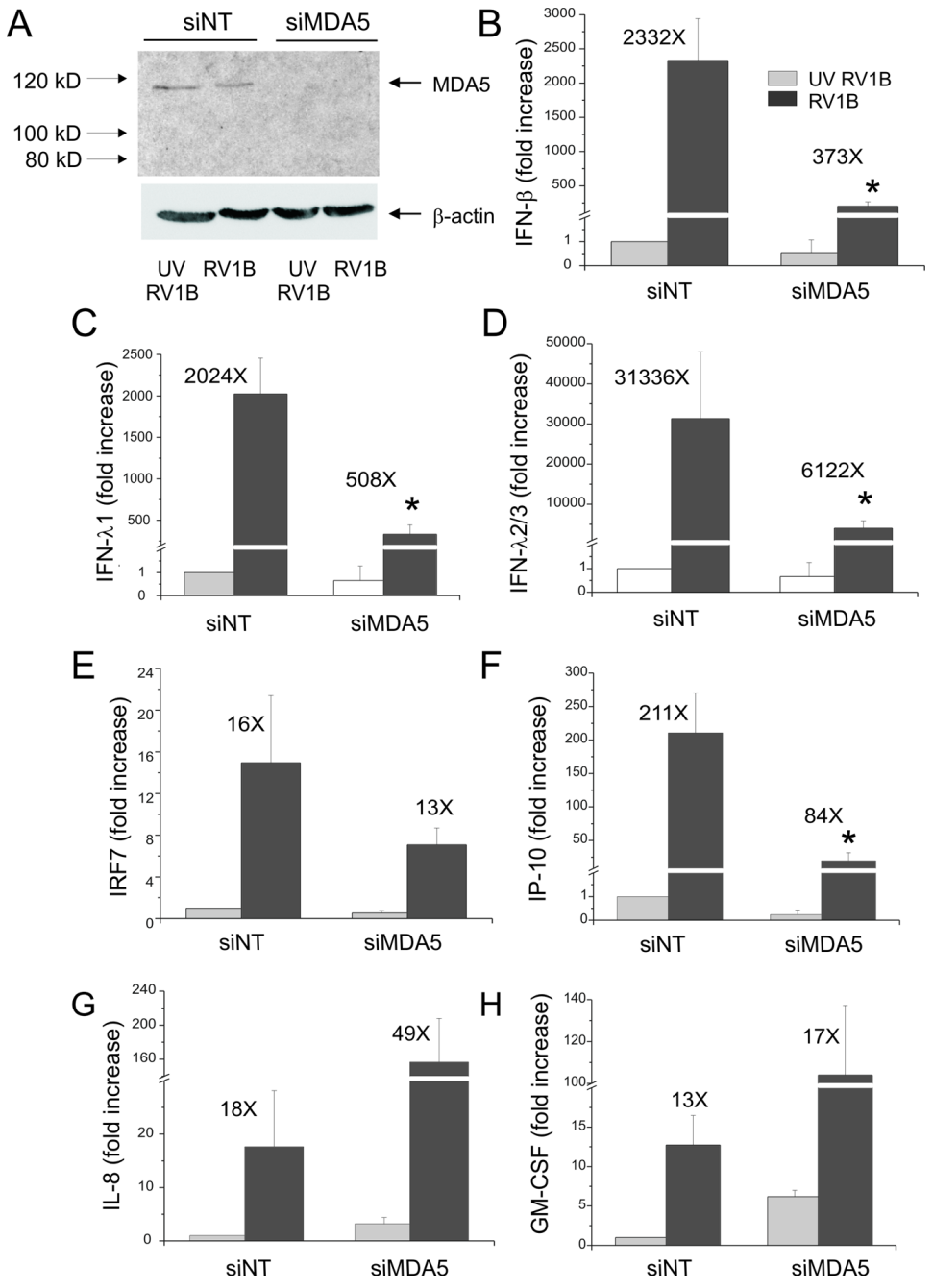

Figure 8. siRNA against MDA5 blocks RV1B-induced IFN responses in primary tracheal epithelial cells

A. MDA5 siRNA or non-targeting siRNA was transfected into primary tracheobronchial epithelial cells. After transfection, cells were infected with RV1B or UV-irradiated RV1B. After infection, cell lysates were probed with anti-MDA5 antibody. The blot shown is typical for three experiments. B–H. Total RNA was extracted and the expression of IFN-β, IFN-λ1, IFN-λ2/3, IRF7, IP-10, IL-8 and GM-CSF was determined by qPCR. The expression of each target gene was normalized to GAPDH. Expression levels are represented as the fold increase vs. cells treated with UV-irradiated virus and non-targeting siRNA. The y-axis has been broken in order to show the effects of siRNA on both basal and

maximal gene expression. Bars represent mean ± SEM for 3 experiments; numbers on top of bars indicate the fold increase compared to sham-infected sample within its own siRNA group. (*p<0.05 vs. MDA5 siRNA-transfected RV-infected sample, ANOVA.)

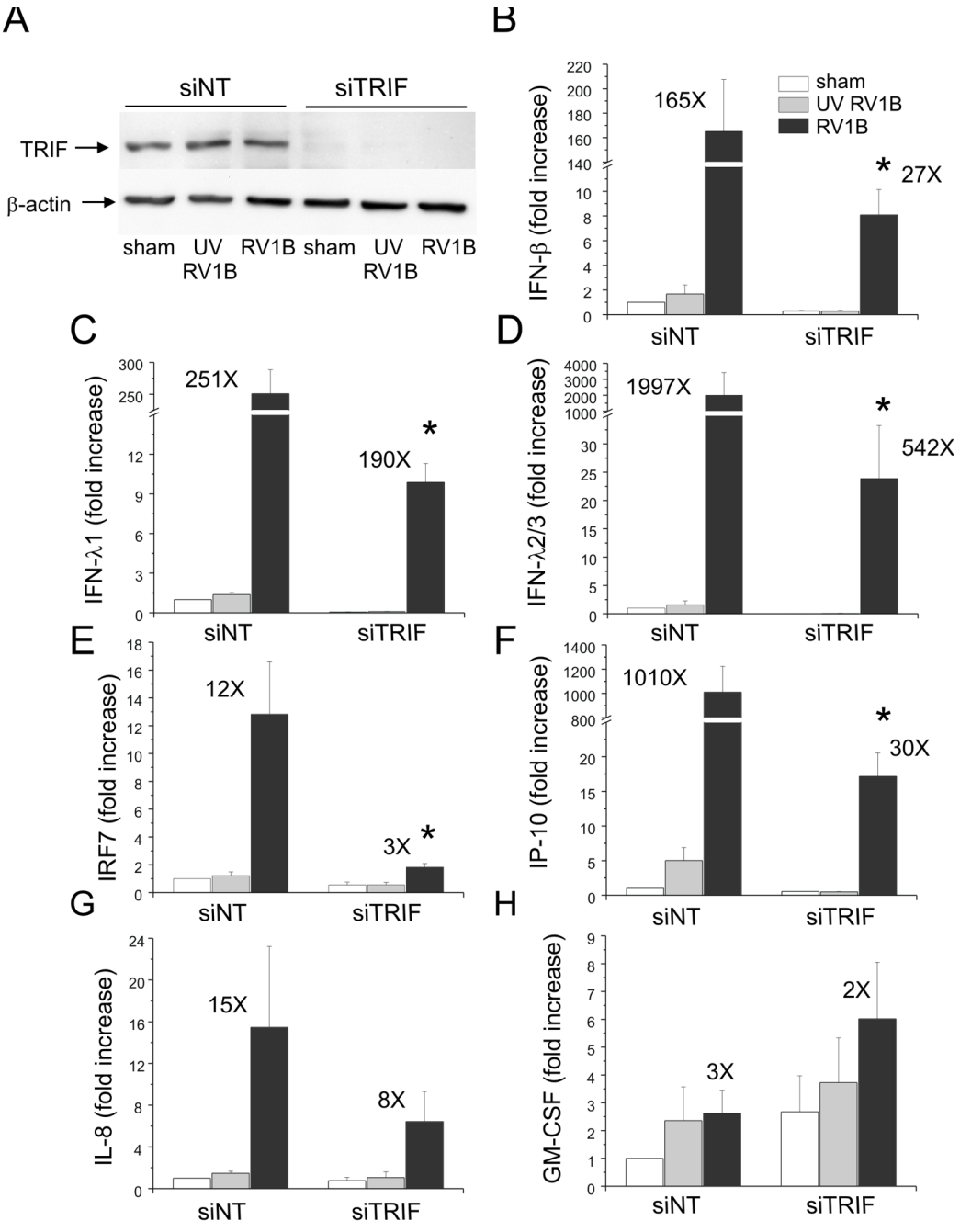

Figure 9. siRNA against TRIF blocks RV-induced IFN and ISG expression

A. TRIF siRNA or non-targeting siRNA was transfected into BEAS-2B cells. After transfection, cells were infected with RV1B, UV irradiated-RV1B or sham. After infection, cell lysates were probed with anti-TRIF antibody. B–H. Total RNA was extracted and the expression of IFN-β, IFN-λ1, IFN-λ2/3, IRF7, IP-10, IL-8 and GM-CSF was determined by qPCR. The expression of each target gene was normalized to GAPDH. Expression levels are represented as the fold increase vs. sham-infected, non-targeting siRNA-transfected cells. The y-axis has been broken in order to show the effects of siRNA on both basal and maximal gene expression. The blot shown is a typical representative of 3 separate experiments. Bars represent mean ± SEM for 4 experiments; numbers on top of bars indicate

the fold increase compared to sham-infected sample within its own siRNA group. (*$p<0.05$ vs. TRIF siRNA-transfected RV-infected sample, ANOVA.)

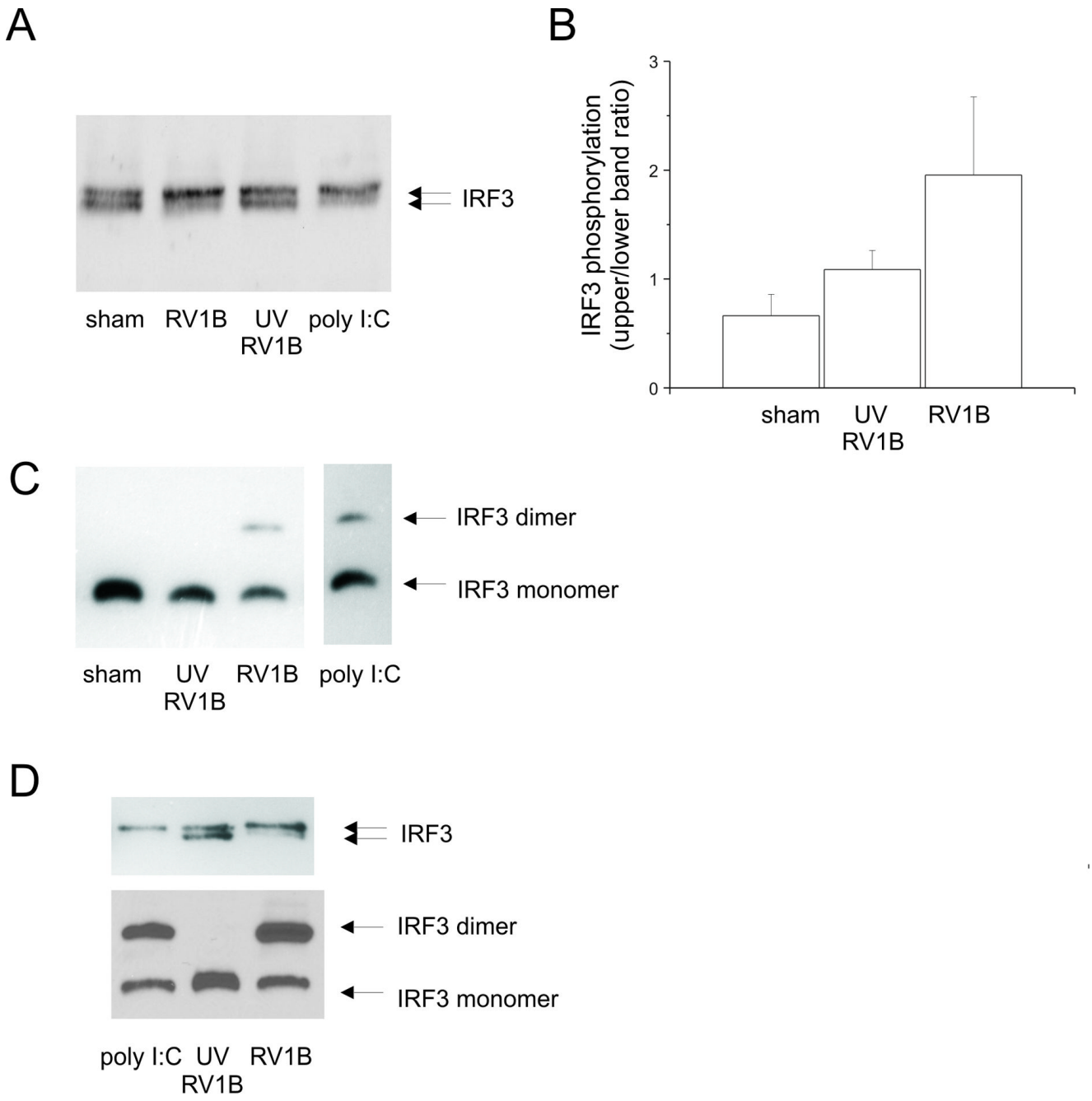

Figure 10. RV-induced IRF3 activation in cultured BEAS-2B and primary airway epithelial cells

A. BEAS-2B cells were infected with RV1B or UV-irradiated RV1B (1 h at 33°C) at MOI=10. Cell lysates were collected and probed with anti-IRF3 antibody. Poly I:C served as a positive control. IRF3 protein is visualized as two bands, an upper phosphorylated form and a lower unphosphorylated form. B. Densitometry of IRF3 phosphorylation is provided. Bars represent mean ± SEM for 3 experiments. C. Cellular proteins were also subjected to native-PAGE to resolve the dimerization of IRF3. Poly I:C served as a positive control. IRF protein is visualized as two bands, an upper dimer and a lower monomer. (The blot shown is a representative of five individual experiments.) D. Primary tracheobronchial epithelial cells were infected with RV1B or UV-irradiated RV1B. Upper panel: cell lysates were collected

twelve h after infection and probed with anti-IRF3 antibody. Poly I:C served as a positive control. Lower panel: cellular proteins were subjected to native-PAGE to resolve the dimerization of IRF3. Poly I:C served as a positive control. (The blots shown are representative of three experiments.)

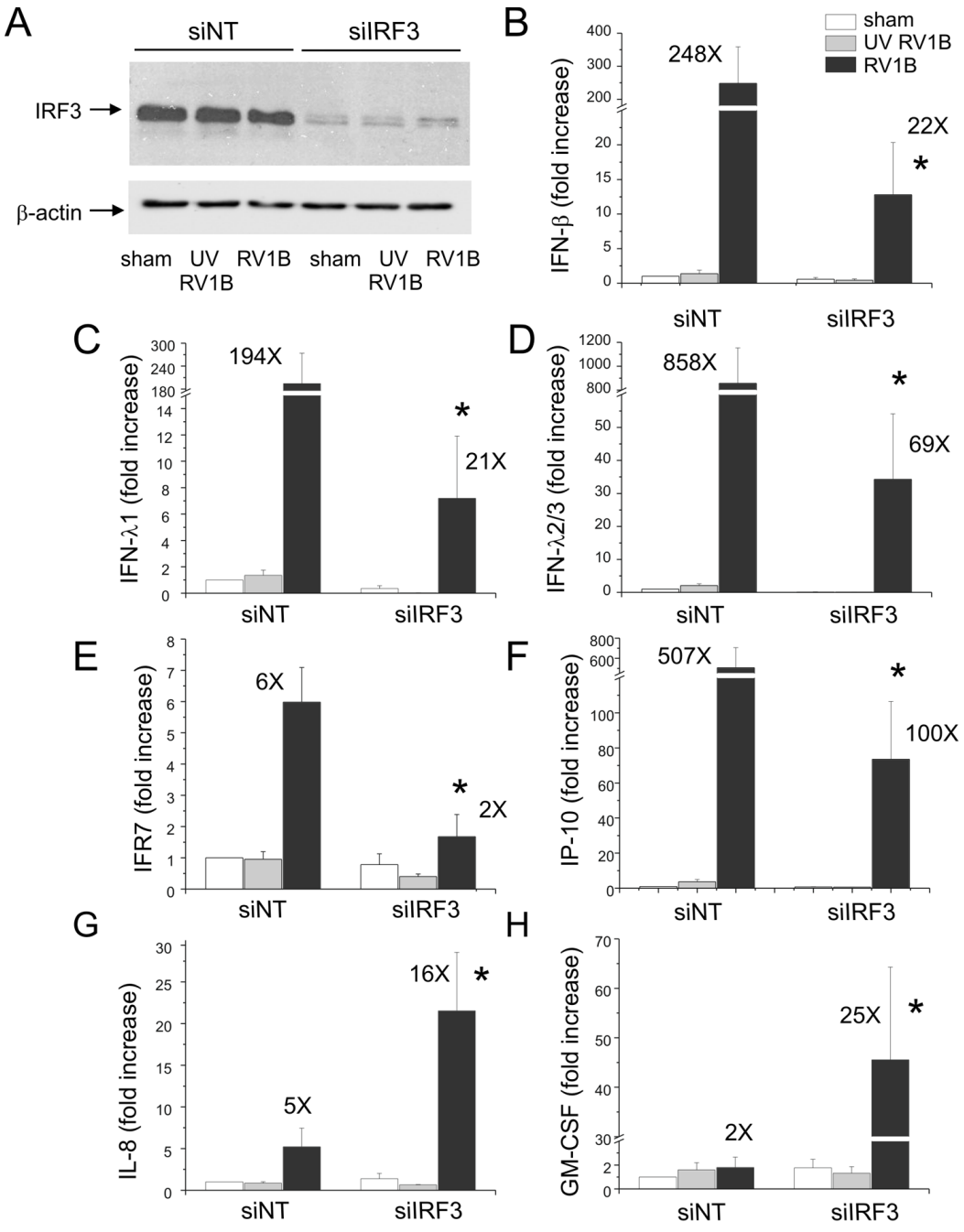

Figure 11. siRNA against IRF3 blocks RV-induced IFN and ISG expression

A. IRF3 siRNA or non-targeting siRNA was transfected into BEAS-2B while seeding. After transfection, cells were infected with RV1B, UV-irradiated RV1B (UV-RV1B) or sham. A. After infection, cell lysates were probed with anti-IRF3 antibody. (The blot shown is representative of 3 separate experiments.) B–H. Total RNA was extracted and the expression of IFN-β, IFN-λ1, IFN-λ2/3, IRF7, IP-10, IL-8 and GM-CSF was determined by qPCR. The expression of each target gene was normalized to GAPDH. Expression levels are represented as the fold increase vs. sham-infected, non-targeting siRNA-transfected cells. The y-axis has been broken in order to show the effects of siRNA on both basal and maximal gene expression. Bars represent mean ± SEM for four experiments; numbers on top

of the bars indicate the fold increase compared to the sham-infected sample within its own siRNA group. (*$p<0.05$ vs. non-targeting siRNA-transfected RV1B-infected cells, one-way ANOVA.)

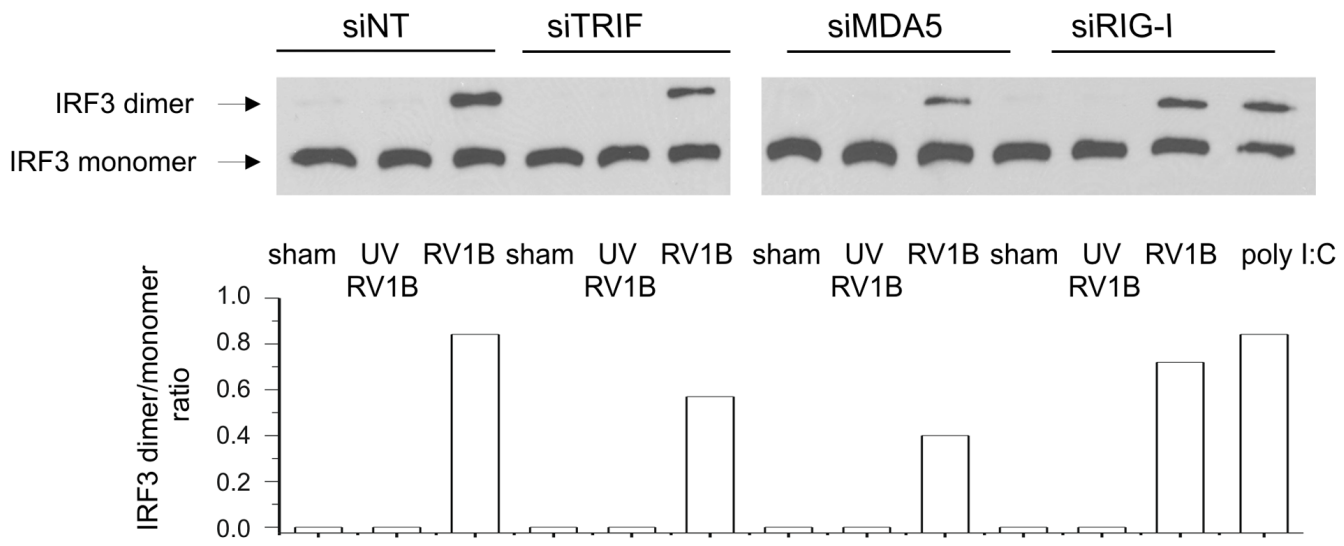

Figure 12. siRNA against TRIF, MDA5, but not RIG-I reduced RV1B-induced IRF3 dimerization

A. RIG-I, MDA5, TRIF siRNA or non-targeting siRNA was transfected into BEAS-2B. After transfection, cells were infected with RV1B, UV-irradiated RV1B or sham. After infection, cell lysates were probed with anti-IRF3 antibody. Poly I:C served as a positive control. B. IRF3 dimer to monomer ratio was quantified by densitometry. (The blot shown is a representative of two experiments.)

Table 1

Effect of RV1B infection on mean cycle threshold (Ct) values of IFN and ISG mRNA expression in BEAS-2B cells.

	sham		RV1B	
	Ct average	**SE**	**Ct average**	**SE**
IFN-β	39.47	0.53	30.91	0.296
IFN-λ1	34.80	0.16	24.23	0.20
IFN-l2/3	39.67	0.33	25.30	0.21
IRF7	24.54	0.20	21.38	0.15
RIG-I	26.97	0.29	21.19	0.19
MDA5	26.50	0.20	21.64	0.11
TLR3	25.47	0.16	22.80	0.04

Table 2

Effect of RV1B infection on mean Ct values of IFN and ISG mRNA expression in primary cells.

	RV1B		sham	
	Ct average	**SE**	**Ct average**	**SE**
IFN-β	35.97	2.14	32.75	2.72
IFN-λ1	33.68	1.69	29.06	2.02
IFN-λ2/3	35.51	1.64	28.47	2.18
IRF7	29.94	1.26	29.87	0.16
RIG-I	28.43	0.31	28.22	0.59
IP-10	30.78	1.00	28.04	0.02